2023 IEEE Wireless and Microwave Technology Conference (WAMICON) | 979-8-3503-9864-9/23/$31.00 ©2023 IEEE | DOI: 10.1109/WAMICON57636.2023.10124898

Gas-Liquid Two-Phase Flow Monitoring Using Sub-THz Radar Imaging

Davi V. Q. Rodrigues
Dept. of Electrical & Computer Engineering
Texas Tech University
Lubbock, TX, 79409, USA
davi.rodrigues@ttu.edu

Daniel Rodriguez
Dept. of Electrical & Computer Engineering
Texas Tech University
Lubbock, TX, 79409, USA
daniel-fernando.rodriguez@ttu.edu

Victor Pugliese
Dept. of Ingeniería Mecánica
Universidad del Norte
Puerto Colombia, ATL, 081008, COL
vpugliese@uninorte.edu.co

Marshall Watson
Dept. of Petroleum Engineering
Texas Tech University
Lubbock, TX, 79409, USA
marshall.watson@ttu.edu

Changzhi Li
Dept. of Electrical & Computer Engineering
Texas Tech University
Lubbock, TX, 79409, USA
changzhi.li@ttu.edu

***Abstract*—Two-phase flow monitoring is widely present in various industrial processes. The most popular methods used to estimate flow parameters can be divided into the noncontact and the contact -based modalities. Conductance-based and capacitive sensors are the most popular contact-based techniques used to provide flow parameter estimations. Among the noncontact sensors, optical-based systems are commonly utilized for multiphase flow classification. However, contact-based systems require specific proprieties from the analyzed fluid mixture such as high conductivity or low conductivity and they must be attached to the tube, so accurate measurements can be provided. On the other hand, optical devices lack robustness against ambient light conditions and might require complex computational processing pipelines. In this work, gas-liquid two-phase flow monitoring based on radar technology is proposed. Characteristic flow velocity distributions associated with different two-phase flows are remotely recognized by studying the reflected sub-THz signals that are phase-modulated by the moving gas-liquid interface. Experimental results confirm the feasibility of the proposed scheme for the identification of different gas-liquid two-phase flows using sub-THz radar imaging.**

Keywords—Doppler radar, gas-liquid flow, multiphase flow monitoring, remote detection, wireless sensing.

I. Introduction

The recognition of flow patterns is crucial to maintain the effectiveness of several procedures in food processing, petroleum, chemical, nuclear, and geothermal industries [1]-[3]. Two-fluid flows are transient and complex systems with random and time-variant flow parameters. Although only one sensing technique cannot provide a comprehensive view of the flow process, either water holdup or fluid speed measurements may be readily available after employing standalone systems such as electrical capacitive tomography or acoustic sensors.

Multiphase flow recognition can be achieved by conductance, capacitive or electromagnetic-based techniques [4]-[7]. Conductance sensors take advantage of the conductivity of the mixed fluids to estimate its flow parameters and requires the continuous phase of the measure fluid to be electrically conductive. However, since the electrodes are in contact with the measured fluid, electrochemical erosion or electrode polarization may lead to measurement errors. In contrast, capacitive sensing architectures are designed to exploit the changes on the permittivity of the fluid mixture and can only provide reliable flow information for nonconductive or low conductive mixture of fluids. Nonetheless, they are highly sensitive to variations in the environment such as temperature or humidity.

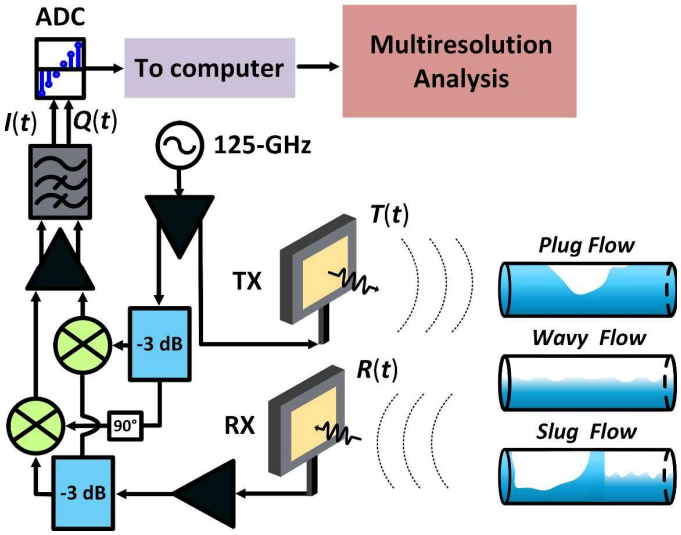

Fig. 1. Block diagram for the proposed gas-liquid two-phase recognition using sub-THz Doppler radar.

Electromagnetic methods include optical, acoustic, and radar devices. Optical devices such as cameras provide flow parameter estimation by measuring changes on the light intensity [7]-[8]. However, these approaches rely on the ambient light conditions and may demand large computational resources for data signal processing. On the other hand, acoustic sensors leverage dispersed scatters (e.g., bubbles) for ultrasound backscattering. The Doppler shifts caused by the relative motion between the scatters and the source of sound signals is proportional to the flow velocity. However, ultrasonic sensors must be properly attached to the tube superficies to avoid false positive results due to the formation of rust.

Radar-based flow monitoring has been proposed for superficial speed estimation of moving fluid and air bubble

detection [9]-[10]. In [10], the instantaneous speed of the air bubble was obtained by analyzing the Doppler shifted received signals that are backscattered by the moving air-liquid interface. Since radar technology relies on radio waves, these sensors do not need to be attached to the tube to provide reliable superficial flow velocity estimations. In contrast to optical sensors, they can be used in dirty environments due to the ability of RF signals to penetrate non-metallic materials such as glass, plastic, fog, and dust. In addition to be a low-cost and easy-to-deploy solution, radar signal processing pipeline is less complex than the data signal processing required by vision-based systems.

In this work, gas-liquid two-phase flow recognition using sub-THz radar imaging is proposed. Different combinations of air and water would lead to different degrees of fluid surface roughness with respect to sub-THz wavelength. The shape of the resultant gas-liquid interface also impacts the measured superficial speed of the moving fluid. Wavelet-based multiresolution analysis of the baseband responses is used to recognize the meaningful Doppler shifts associated with three gas-liquid two-phase flows. A series of experimental results are presented to demonstrate the performance of the proposed approach.

II. Theory

The block diagram for the gas-liquid two-phase flow monitoring based on sub-THz radar imaging is shown in Fig. 1. The radar system consists of a typical 125-GHz Doppler radar. The sensor transmits signals towards the mixture of gas and liquid that moves inside the tube. Upon encountering changes on the propagation medium (gas-liquid interface), part of the electromagnetic (EM) waves is backscattered towards the radar's receiving antenna. Since there is a relative motion between the radar system and the moving gas-liquid phase, the received signals are phase-modulated because of the Doppler effects. The frequency-shift is proportional to the radial speed of gas-liquid interface. After amplification, the captured received signals are down-converted to baseband.

Due to the complex nature of two-phase flows, the radar-cross section (RCS) of the gas-liquid interface and its corresponding speed may vary randomly. Therefore, the down-converted received signals will be a mixture of several spectral components that may appear in different time instances. It is important to separate these components and examine them individually under the same time scale of the original signal. The most meaningful spectral components can used to identify different flows. To further gain insight on the recovered I/Q baseband signals and study the signal variations associated with meaningful physical phenomena, the extraction of the signal components at different frequency bands is needed. To do so, a multiresolution analysis (MRA) technique based on the maximal overlap discrete wavelet transform (MODWT) is utilized to study the variations on the received radar signals for the recording of gas-liquid flows. The symlet 4 wavelet is chosen as the scaling function for the MRA of the amplitude of the complex-valued baseband signals, i.e., $|I(t) + jQ(t)|$. It should be noted that the MODWT-based MRA is regarded as a

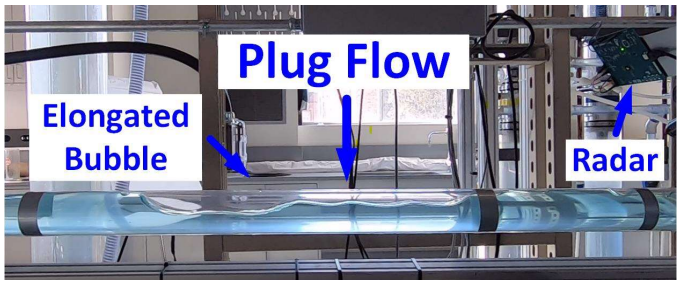

Fig. 2. Experimental setup. Radar-based recognition of plug flow.

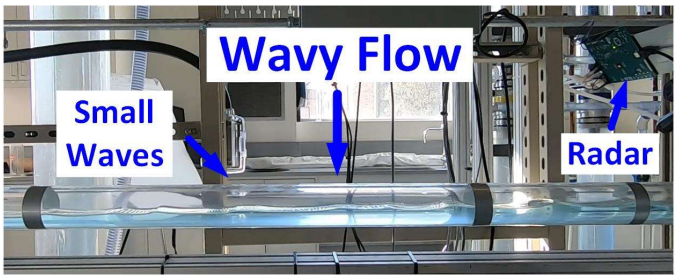

Fig. 3. Experimental setup. Radar-based recognition of wavy flow.

Fig. 4. Experimental setup. Radar-based recognition of slug flow.

zero-phase filtering of the analyzed signal into frequency bands with the form $[f_s/2^{i+1}, f_s/2^i]$, where f_S is the sampling frequency, $i \in \mathbb{N}$, $1 \leq i \leq L$, is associated with i-th wavelet MRA component. After applying L-th MODWT-based MRA to $|I(t) + jQ(t)|$, a coarse signal's approximation S_L and L other MRA components $D_j, j = 1, 2, 3, \ldots, L$, also known as j-level detail coefficients, will be generated [11].

III. Experimental Results

A series of field experiments were done to evaluate the feasibility of the proposed application. The test facility was a closed horizontal flow loop located at the Terry Fuller Petroleum Engineering Research Building at Texas Tech University. Fig. 2, Fig. 3, and Fig. 4 show the experimental setups for the sub-THz radar imaging of plug flow, wavy flow, and slug flow, respectively. The 125-GHz Doppler radar was mounted on a tripod, the distance between the radar sensor and the tube was 25 cm, and the radar board was tilted by 45° with respect to a vertical line. The tube is made of transparent acrylic resin with outer diameter of 6.35 cm and inner diameter of 5.08 cm. The ac-coupled 125-GHz Doppler radar was designed using the Silicon Radar TRX_120_001 on-chip frontend. The gains of the transmitting and receiving antennas are around 9 dB and 10 dB, respectively, and the output power of the radar's

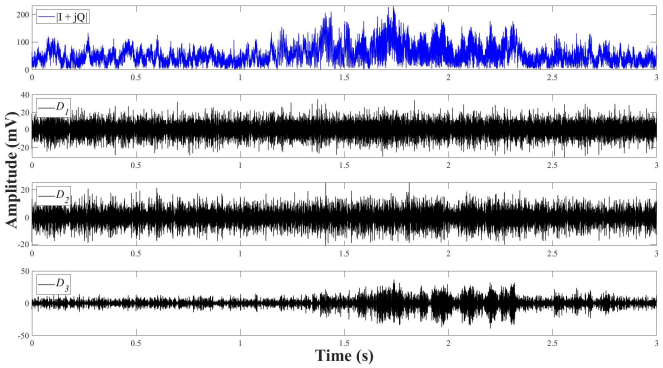

Fig. 5. Multiresolution analysis for the radar recording of plug flow. The amplitude of the complex-valued I/Q baseband signals and the corresponding detail coefficients from the first up to the third level are shown from top to bottom, respectively.

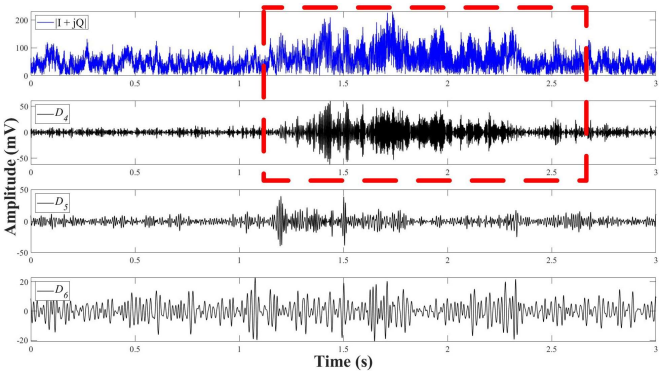

Fig. 6. Multiresolution analysis for the radar recording of plug flow. The amplitude of the complex-valued I/Q baseband signals and the corresponding fourth, fifth, and sixth-level detail coefficients are shown from top to bottom, respectively.

transmitter is -3 dBm. The baseband outputs were digitized using a 16-bit analog-to-digital converter (ADC) DI-2108 designed by DATAQ with a sampling frequency f_s set to 5-kS/s.

To form different flow patterns, atmospheric air and water were pumped into the tube at different mass flow rates. A LabVIEW platform was used to control the mass flow for the gas and liquid phases. For the plug flow, the mass flow rate for the liquid phase was measured as 111 g/s while the mass flow rate for the air phase was calculated as 0.008 g/s. For the wavy flow, the water's mass flow rate was adjusted to 0.446 g/s and the air's mass flow rate was changed to 3.72 g/s. Finally, for the slug flow, the water's mass flow rate was 111 g/s while the air's mass flow rate was set to 6.56 g/s.

The amplitude of the complex-valued recorded radar signals was decomposed in fourteen levels of wavelet-based decomposition $(L = 14)$. The first six levels of wavelet decomposition are associated with the following frequency bands [625 Hz, 1250 Hz], [312.5 Hz, 625 Hz], [156.25 Hz, 312.5 Hz], [78.125 Hz, 156.25 Hz], [39.0625 Hz, 78.125 Hz], and [19.53125 Hz, 39.0625 Hz]. Fig. 5 depicts four subplots associated with the radar recordings of plug flow. From top to bottom, the first subplot is the amplitude of the complex-valued signal $I + jQ$. The second subplot is the first-level wavelet

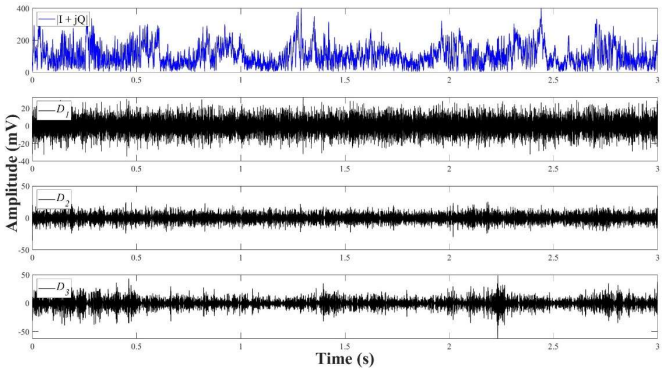

Fig. 7. Multiresolution analysis for the radar recording of wavy flow. The amplitude of the complex-valued I/Q baseband signals and the corresponding detail coefficients from the first up to the third level are shown from top to bottom, respectively.

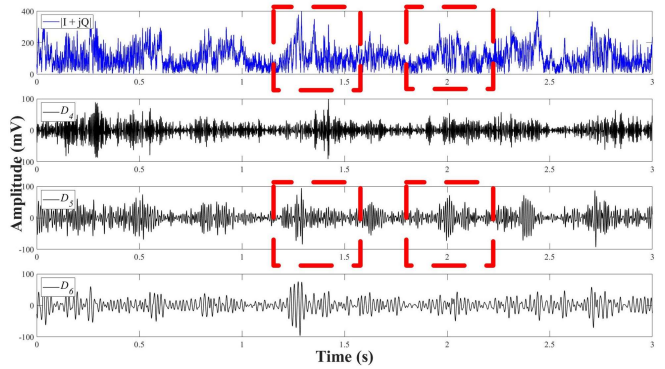

Fig. 8. Multiresolution analysis for the radar recording of wavy flow. The amplitude of the complex-valued I/Q baseband signals and the corresponding fourth, fifth, and sixth-level detail coefficients are shown from top to bottom, respectively.

detail coefficients (D_1), while the third and fourth subplots are the second and third-level detail coefficients (D_2, D_3), respectively. Similarly, in Fig. 6, the amplitude of the complex baseband signals, and the fourth, fifth, and sixth-level detail coefficients (D_4, D_5, D_6) for the radar recording of a plug flow are shown from top to bottom, respectively. As seen in Fig. 2, for a plug flow, an elongated bubble moves along the tube. Since changes on the gas-liquid interface are observed, a portion of the emitted EM energy is backscattered towards the radar. The moving elongated bubble causes Doppler shifts on the sub-THz transmitted signals. On the other hand, when no elongated bubble travels through the radar's field of view, no changes can be seen on the gas-liquid interface and a smooth surface is created. As a consequence, most of the incident EM waves are reflected in the specular direction or absorbed by the liquid phase and no Doppler shifts is observed on the received sub-THz signals. It should be noted that the frequencies of the spectral components become progressively lower through D_1 to D_6, and the relevant or dominant signal features are isolated in fourth-level detail coefficients (D_4) for the radar recording of plug flow.

Fig. 7 shows the amplitude of the complex-valued recovered I/Q baseband signals and the first, second, and third-level detail coefficients (D_1, D_2, D_3) for the radar recording of

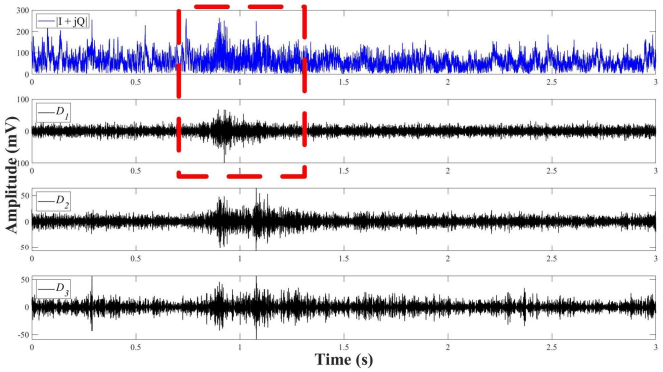

Fig. 9. Multiresolution analysis for the radar recording of slug flow. The amplitude of the complex-valued I/Q baseband signals and the corresponding detail coefficients from the first up to the third level are shown from top to bottom, respectively.

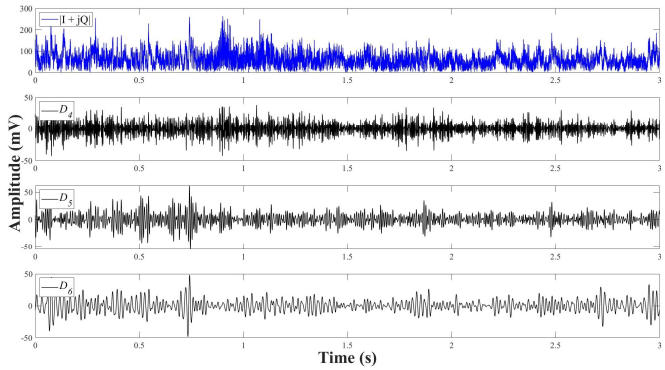

Fig. 10. Multiresolution analysis for the radar recording of slug flow. The amplitude of the complex-valued I/Q baseband signals and the corresponding fourth, fifth, and sixth-level detail coefficients are shown from top to bottom, respectively.

the wavy flow. Fig. 8 exhibits the fourth, fifth, and sixth-level (D_4, D_5, D_6) detail coefficients for the radar recording of the wavy flow. The relevant feature for the wavy flow is the appearance of small perturbations followed by an almost flat surface on the gas-liquid interface that move uniformly. Therefore, relatively lower frequency components of short duration associated with the fluid's superficial speed and zero-Doppler spectral components associated with the smooth surface (in this order) are expected to be found on the recovered baseband signals. As highlighted in Fig. 8, the key features of sub-THz radar signals that are associate with wavy flow are summarized by the fifth-level detail coefficients (D_5).

Fig. 9 reveals the amplitude of the complex-valued down-converted I/Q signals and the first three corresponding wavelet-based detail coefficients for the slug flow. Besides the amplitude of the complex baseband signals, Fig. 10 shows the fourth, the fifth, and the sixth level wavelet-based detail coefficients for the radar recording of the slug flow. In the slug flow regime, the shape of the gas-liquid interface vary dramatically because of the rapid appearance of a slug body, which also carries bubbles with high speed. Therefore, an energetic instantaneous Doppler shift associated with the abrupt changes on the liquid's superficial speed is observed on the recovered baseband signals as highlighted in Fig. 9. The most meaningful statistical features associated with the radar recording of the slug flow (powerful high frequency spectral components) are isolated in the first-level detail coefficients (D_1).

IV. Conclusion

This paper investigated the feasibility of using a sub-THz Doppler radar for two-phase flow monitoring. The MRA of the radar recording for three different combinations of the air and water, i.e., plug flow, wavy flow, and slug flow, were studied. By decomposing the recovered baseband radar responses in various frequency bands, different spectral distributions associated with different combination of moving gas and liquid phases are simultaneously analyzed both in time and frequency domains. Furthermore, the key/dominant spectral feature for a specific two-phase flow is isolated in one of calculated MRA components. Future research will focus on the design of a machine learning-based algorithm for multiphase flow classification using sub-THz radar signatures.

Acknowledgment

The authors wish to acknowledge National Science Foundation (NSF) for funding support under the Grant 1808613 and the Grant 2030094.

References

[1] H. Wang, D. Hu, M. Zhang, N. Li and Y. Yang, "Multiphase flowrate measurement with multi-modal sensors and temporal convolutional network," *IEEE Sensors J.* (early access).

[2] Z. Gao, W. Dang, C. Mu, Y. Yang, S. Li and C. Grebogi, "A Novel Multiplex Network-Based Sensor Information Fusion Model and Its Application to Industrial Multiphase Flow System," *IEEE Trans. Industr. Inform.,* vol. 14, no. 9, pp. 3982-3988, Sept. 2018

[3] R. K. Rasel, C. E. Zuccarelli, Q. M. Marashdeh, L. -S. Fan and F. L. Teixeira, "Toward Multiphase Flow Decomposition Based on Electrical Capacitance Tomography Sensors," *IEEE Sensors J.*, vol. 17, no. 24, pp. 8027-8036, 15 Dec.15, 2017.

[4] D. Wang, N. Jin, L. Zhai and Y. Ren, "Measurement of Gas Holdup in Oil-Gas-Water Flows Using Combined Conductance Sensors," *IEEE Sensors J.*, vol. 21, no. 10, pp. 12171-12178, 15 May15, 2021

[5] A. D. N. Wrasse, D. Bertoldi, E. N. Dos Santos, R. E. M. Morales and M. J. Da Silva, "Gas–Liquid Flow Rate Measurement Using a Twin-Plane Capacitive Sensor and a Venturi Meter," *IEEE Access*, vol. 7, pp. 135933-135941, 2019.

[6] N. A. Zulkiflli *et al*., "Ultrasound Tomography Hardware System for Multiphase Flow Imaging," *IEEE International Conference on Signal and Image Processing Applications (ICSIPA)*, Kuala Lumpur, Malaysia, 2019

[7] M. Jia, W. Zhou, N. Jin and X. Cai, "A measuring method for 3-D movement of particles using single-lens dual-camera system," *IEEE International Conference on Imaging Systems and Techniques (IST)*, Chania, Greece, 2016, pp. 135-139.

[8] C. R. Zamarreno *et al*., "Single and Multiphase Flow Characterization by Means of an Optical Fiber Bragg Grating Grid," *J. Light. Technol*., vol. 33, no. 9, pp. 1857-1862, May, 2015.

[9] T. Wang, S. Hao and X. Ma, "Water Velocity and Level Monitoring Based on UAV Radar," *IEEE 4th Advanced Information Management, Communicates, Electronic and Automation Control Conference (IMCEC),* Chongqing, China, 2021, pp. 1232-1236.

[10] D. V. Q. Rodrigues, D. Rodriguez, V. Pugliese, M. Watson and C. Li, "Air Bubble Detection Based on Portable mm- Wave Doppler Radars," *IEEE MTT-S International Wireless Symposium (IWS)*, Nanjing, China, 2021, pp. 1-3

[11] D.B. Percival, and A.T. Walden, "Wavelet Methods for Time Series Analysis". Cambridge Series in Statistical and Probabilistic Mathematics; Cambridge University Press: New York, NY, USA, 2000.